Self-Aggregation Inhibits the Photonuclease Activity of Porphyrins

Katsumasa AOKI, Yoshinobu ISHIKAWA, Miyuki OYAMA, Yoshikazu TOMISUGI, and Tadayuki UNO*

Faculty of Pharmaceutical Sciences, Kumamoto University; Oehonmachi, Kumamoto 862–0973, Japan.
Received December 16, 2002; accepted June 13, 2003; published online June 13, 2003

A series of tentacle porphyrins having four aminoalkyl groups at the periphery was synthesized, and the DNA binding properties were investigated by absorption and circular dichroism (CD) spectroscopic methods. The aminopropyl chain was found to facilitate binding, and bisignate induced CD spectra revealed that the porphyrins are self-stacked on the DNA surface. The photonuclease activity of the tentacle porphyrins was also studied, and the aminopropylporphyrin showed the highest activity. The activity increased in proportion to the porphyrin load, but higher loads resulted in the decrease of activity. This inhibitory step corresponded to aggregation of the porphyrin. Thus, the aggregation was suggested to shield the inner porphyrin from the solvent, the production of active oxygen species being suppressed.

Key words photonuclease; porphyrin; aggregation; DNA; active oxygen

The development of efficient and DNA-specific photosensitizers attracts much attention in the growing field of cancer photodynamic therapy (PDT).[1,2] In these applications, the photosensitizers bind to DNA specifically, generate active oxygen species upon illumination, and subsequently cleave DNA in malignant cells. The DNA damage will disturb the genetic events and thus the proliferation of tumor cells is suppressed. Therefore, both tight binding to DNA and efficient generation of active oxygen species are prerequisites for an effective PDT reagent.

Porphyrins can be effective photosensitizers, and anionic Photofrin, a purified fraction of an oligomeric hematoporphyrin derivative (HPD),[3,4] is now clinically used in cancer PDT.[5] From the view point of DNA targeting, cationic porphyrins have been studied extensively, because of their potential for electrostatic binding to DNA.[6—8] Three major modes have been proposed for porphyrin binding: intercalation, outside binding in the groove, and outside binding with self-stacking along the DNA surface.[9] These binding modes can be revealed by various techniques such as UV–visible absorption,[9—11] circular dichroism (CD),[9—12] fluorescence,[13,14] NMR,[15,16] and resonance Raman[17,18] spectroscopies.

We have recently prepared zinc complexes of cationic porphyrins, and shown that metal insertion into the porphyrin core drastically enhances the photonuclease activity of the porphyrin.[19] The evidence suggests strongly that the active species is singlet oxygen,[19] since the activity was proportional to the singlet oxygen productivity of the porphyrins, and scavengers of this molecule greatly reduced the activity.

As well as the enhanced generation of the active oxygen, refined control of the mode of binding is required in order to maximally enhance the photonuclease activity of porphyrins. The relationship between the photonuclease activity and the binding modes is not yet fully understood. In the course of intensive studies on porphyrin photonuclease activities,[19—21] we have found that highly aggregative porphyrins tend to have lower activities. We therefore synthesized a series of tentacle porphyrins having four aminoalkyl chains (Fig. 1). By correlating the binding properties with photonuclease activities, we have shown that self-aggregation is an inactive mode of binding. This result provides a clue to the future development of porphyrin-based photosensitizers applicable to PDT.

Experimental

Instrumentation The ^{1}H-NMR spectra were recorded on a JEOL GX-400 or JNM-A-500 spectrometer. Matrix-assisted laser desorption ionization time-of-flight (MALDI-TOF) mass spectra were measured on a Bruker REFLEX. The UV–visible absorption measurement was performed on a Beckman DU640 spectrophotometer. The CD spectra were recorded on a JASCO J-720 spectropolarimeter. Elemental analyses were performed at the Center for Instrumental Analysis, Kumamoto University.

Materials and Methods Tetrakis(4-aminophenyl)porphine (TAPP) and reagents for the synthesis of tentacle porphyrins were purchased from Tokyo Chemical Industry, Wako Pure Chemicals, and Dojin. Calf thymus (ct) DNA was purchased from Sigma, and pUC18 plasmid DNA from Stratagene. The DNA solution was quantitated spectrophotometrically using $\varepsilon_{260}=13.2$ mM^{-1} cm^{-1}, and the concentrations of DNA were expressed in terms of base pairs.

Synthesis of Porphyrins Twenty millimoles of amino acid (4-amino-*n*-butyric acid, 6-aminohexanoic acid, and *ω*-aminocaprylic acid) was dissolved in water (11 ml) and triethylamine (30 mmol), and dioxane solution (11 ml) of 2-BOC-thio-4,6-dimethylpyrimidine (22 mmol, BOC=butyloxycarbonyl) was poured. After stirring for 26 h at room temperature, 30 ml of water was poured and unreacted materials were removed with ethyl acetate. The water layer was brought to pH 2 with HCl on ice, and BOC-protected amino acid was extracted with ethyl acetate. The extract was washed with ice-cold 5% HCl and then with saturated NaCl, and dried over anhydrous sodium sulfate. The solvent was removed and product was obtained as oil (BOC-amino-*n*-butyric acid and BOC-aminohexanoic acid) or as powder (BOC-aminocaprylic acid). The yield commonly amounted to more than 80%.

The BOC-amino acid (3 mmol) and 1-ethyl-3-(3-dimethylaminopropyl)-carbodiimide (3 mmol) were dissolved in dimethylformamide (DMF) and stirred for 1 h. TAPP (0.15 mmol) and 1-hydroxybenzotriazole (3 mmol) were added and stirred overnight. Chloroform (200 ml) was poured into the mixture, washed three times with water, and the organic layer was dried over anhydrous sodium sulfate. In the case of BOC-aminocaprylic acid, unreacted materials were separated by silica gel chromatography (methanol/$CHCl_3$=50/50). The solvent was removed and trifluoroacetic acid (TFA) was poured onto the residue. The amino group was deprotected stirring for 1 h on ice.

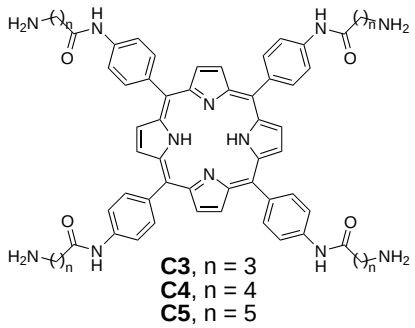

Fig. 1. Tentacle Porphyrins Synthesized in This Study

* To whom correspondence should be addressed. e-mail: unot@gpo.kumamoto-u.ac.jp

The product was precipitated by pouring diethylether, filtered, and dissolved in minimal amount of methanol. When the solution was green, triethylamine was added until the color turns to purple. Addition of diethylether to the solution and slow diffusion gave a purple powder, which was collected and dried.

Tetrakis[4-(4-aminobutanamido)phenyl]-porphine (**C3**): Yield: 28%. ^{1}H-NMR (CD_3OD) δ: 2.15 (8H, m), 2.75 (8H, t), 3.15 (8H, t), 8.10 (16H, dd), 8.89 (8H, br). UV λ_{max} (DMF) nm (ε): 423 (478000), 519 (19600), 556 (16400), 594 (6590), 652 (9120). MALDI-TOF-MS *m*/*z*: 1015.3 (M^+, Calcd for $C_{60}H_{62}N_{12}O_4$: 1015.2). *Anal.* Calcd for $C_{60}H_{62}N_{12}O_4 \cdot 4CF_3COOH$: C, 55.50; H, 4.53; N, 11.43. Found: C, 55.50; H, 4.81; N, 11.70.

Tetrakis[4-(4-aminohexanamido)phenyl]-porphine (**C5**): Yield: 64%. ^{1}H-NMR (CD_3OD) δ: 1.61 (8H, m), 1.80 (8H, m), 1.89 (8H, m), 2.62 (8H, t), 3.02 (8H, t), 8.09 (16H, dd), 8.91 (8H, br). UV λ_{max} (DMF) nm (ε): 423 (408000), 520 (18200), 558 (15800), 595 (6720), 652 (8100). MALDI-TOF-MS *m*/*z*: 1127.2 (M^+, Calcd for $C_{68}H_{78}N_{12}O_4$: 1127.4). *Anal.* Calcd for $C_{68}H_{78}N_{12}O_4 \cdot 4CF_3COOH$: C, 57.65; H, 5.22; N, 10.61. Found: C, 57.50; H, 5.02; N, 10.28.

Tetrakis[4-(4-aminooctanamido)phenyl]-porphine (**C7**): Yield: 32%. ^{1}H-NMR (CD_3OD) δ: 1.53 (24H, m), 1.73 (8H, m), 1.88 (8H, m), 2.62 (8H, t), 2.97 (8H, t), 8.40 (16H, dd), 8.81 (8H, s). UV λ_{max} (DMF) nm (ε): 423 (493000), 519 (18500), 556 (15600), 594 (5890), 651 (8090). MALDI-TOF-MS *m*/*z*: 1239.9 (M^+, Calcd for $C_{76}H_{94}N_{12}O_4$: 1239.7). *Anal.* Calcd for $C_{76}H_{94}N_{12}O_4 \cdot 4CF_3COOH$: C, 59.50; H, 5.83; N, 9.91. Found: C, 59.13; H, 6.29; N, 9.94.

Spectral Measurements Aliquots of ctDNA solution were added to the porphyrin solution (*ca.* 2 μM), and absorption spectra were measured at 25 °C in 10 mM sodium phosphate and 30% DMF (pH 7.0). Since the porphyrin solubility was low in water, addition of DMF was necessary. The amount of 30% DMF does not affect the secondary structure of DNA, as judged by CD spectroscopy. The binding constant (*K*) and the number of binding sites per base pair (*n*) were estimated from the spectral changes, following Scatchard analysis.[22—24] The induced CD spectra of the porphyrins (*ca.* 2 μM) were measured at selected concentrations of DNA, and twenty independent spectra were averaged. Conversely, aliquots of the porphyrin solution were added to a DNA solution (*ca.* 30 μM), and four independent CD spectra in the UV range were averaged. The CD spectra were baseline corrected and smoothed.

Photonuclease Assay Photoillumination was performed at 25 °C using a Hitachi 650-60 fluorescence spectrophotometer equipped with a 150 W Xe lamp.[19—21] A sample containing supercoiled pUC18 plasmid DNA and a porphyrin was illuminated in 10 mM sodium phosphate (pH 7.0) and 30% DMF at 420 nm. After illumination, DNA was analyzed by 0.8% agarose gel electrophoresis. The DNA was stained by ethidium bromide and the DNA bands were visualized by fluorescence over a UV lamp. The densitometric data of the bands were obtained with NIH Image software.[25] The staining intensity of relaxed plasmid DNA was found to be 1.5 times that of supercoiled DNA.[26] The band density was corrected based on this difference.

Results

Absorption Spectra In order to evaluate the DNA binding properties of the porphyrins, we first titrated the porphyrin with ctDNA and recorded the absorption spectral change. A typical set of spectra for **C3** is shown in Fig. 2. It is clear that the strong Soret peak at 421 nm decreases greatly upon addition of DNA, indicating that the porphyrin π electrons are perturbed considerably by the DNA binding. Since one set of isosbestic points are clearly observed, the binding appears to take place in a single step. The main Soret peak is blue-shifted with a shoulder at about 430 nm in the presence of large amount of DNA. The spectral properties of **C3**, **C5**, and **C7** are summarized in Table 1. The large hypochromicity (*H*), as well as the large blue shift ($\Delta\lambda$) of the Soret band is distinct from any other porphyrins thus far examined.[24]

Normalized absorbance changes are plotted against the concentration of base pairs in Fig. 3. Since the spectral change takes place in a single step, the binding constant (*K*) and the number of binding sites (*n*) can be estimated successfully (Table 2). Theoretical curves using these *K* and n_{AB} values were found to fit nicely to the absorbance changes actually observed (Fig. 3). It is clear that the **C3** porphyrin has very large *K* value, while n_{AB} value increases as the alkyl chain becomes long. The large *K* value suggests that the chain length of **C3** is appropriate for the binding to DNA.

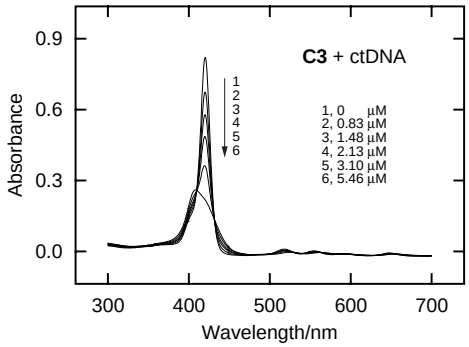

Fig. 2. Absorption Spectral Change of **C3** on the Addition of CtDNA

The porphyrin concentration was 1.72 μM. The spectra were recorded in 10 mM sodium phosphate (pH 7.0) and 30% DMF. Concentrations of DNA were as follows: 1, 0 μM; 2, 0.83 μM; 3, 1.48 μM; 4, 2.13 μM; 5, 3.10 μM; 6, 5.46 μM.

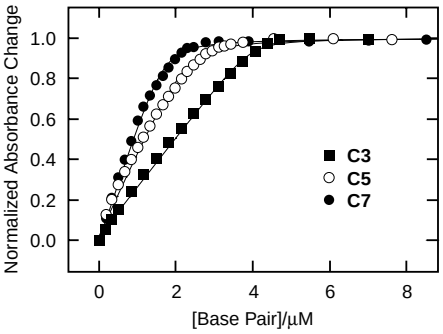

Fig. 3. Normalized Absorbance Change of Tentacle Porphyrins at 421 nm by the Addition of CtDNA

Closed squares, **C3**; open circles, **C5**; closed circles, **C7**. Theoretical solid lines were drawn with the *K* and n_{AB} values in Table 2.

Table 1. Spectral Comparison among Tentacle Porphyrins Bound to CtDNA

Porphyrin	$\Delta\lambda$/nm[a]	*H*/%[b]	Induced CD/nm[c]	
C3	−12	68	393 (−17.5)	405 (+24.7)
C5	−16	72	393 (−11.2)	405 (+18.1)
C7	−11	73	389 (−1.6)	404 (+4.0)

a) Bathochromic shift. *b*) The hypochromicity (*H*/%) was determined by the equation $H=(\varepsilon_f-\varepsilon_b)/\varepsilon_f\times100$, where ε_f and ε_b represent the molar absorptivities of free and bound porphyrins, respectively, which were determined at the respective Soret maxima. *c*) Induced CD peaks. The values in parentheses are molar ellipticities ($[\theta]/10^4$ deg cm^2 dmol^{-1}).

Table 2. Comparison of Binding Parameters among Tentacle Porphyrins

Porphyrin	$K/\mu M^{-1}$	n_{AB}[a]	n_{CD}[b]
C3	96	0.43	0.41 0.17
C5	24	0.64	0.67 0.15
C7	25	0.84	0.84

a) The n_{AB} values obtained from the absorbance changes. *b*) The n_{CD} values obtained from the elliptic changes.

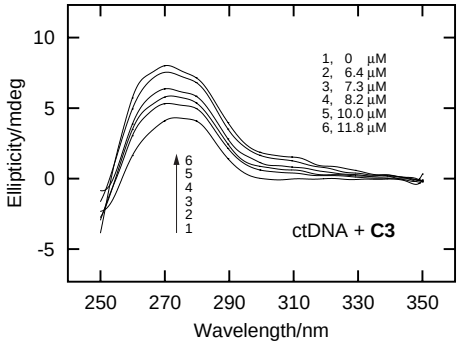

Fig. 4. CD Spectral Changes of CtDNA upon Addition of **C3**

DNA concentration was 27.9 μM. The spectra were recorded in 10 mM sodium phosphate (pH 7.0) and 30% DMF. The concentrations of **C3**: 1, 0 μM; 2, 6.4 μM; 3, 7.3 μM; 4, 8.2 μM; 5, 10.0 μM; 6, 11.8 μM.

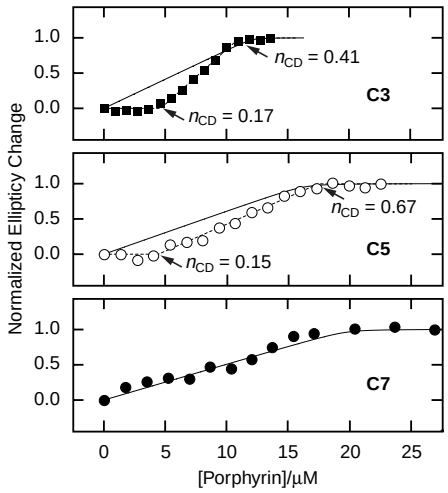

Fig. 5. Normalized Changes in Ellipticity of CtDNA at 260 nm upon Addition of Tentacle Porphyrins

The base pair concentrations were 27.9 μM for **C3**, 25.5 μM for **C5**, and 23.4 μM for **C7**. Closed squares, **C3**; open circles, **C5**; closed circles, **C7**. The solid lines were drawn with the K and n_{AB} values in Table 2. The dashed lines were drawn with the linear part of the ellipticity changes. The break points were marked with arrows.

CD Spectra As we pointed out previously,[24] absorption spectroscopy occasionally fails to detect a binding step if the associated spectral change is small. As an additional approach we employed CD spectroscopy which is sensitive to conformational change in DNA. The CD spectral changes upon **C3** binding are shown in Fig. 4. A strong signal arising from the solvent, DMF, overlaps in the wavelength range below 250 nm, thus the spectra were measured between 250—350 nm. In this range, the spectral change was small, with no obvious shift being observed. Thus, any conformational change in the DNA is likely to be small, *i.e.*, the bound porphyrins interact with DNA without greatly perturbing its structure.

The changes in ellipticity were normalized and plotted against the concentration of porphyrins (Fig. 5). The solid lines illustrate theoretical plots obtained using the K and n_{AB} values obtained from the absorbance data (Table 2). The theoretical curve for **C7** is in good agreement with the observed changes in ellipticity. This indicates that binding proceeds in a single step, and that the absorbance and CD changes inform on the same binding process. In the case of **C3** and **C5**, however, the observed ellipticity plots deviate considerably

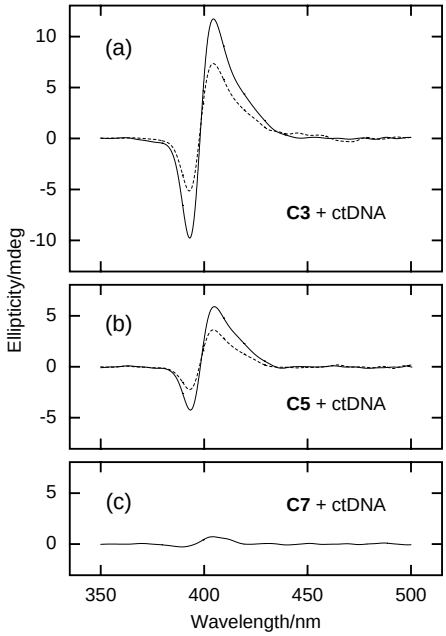

Fig. 6. Induced CD Spectra of Tentacle Porphyrins by the Addition of CtDNA

The spectra were recorded in 10 mM sodium phosphate (pH 7.0) and 30% DMF. (a) **C3**, 2.94 μM; DNA, 7.42 μM (r=0.40, solid line) and 15.0 μM (r=0.20, dashed line). (b) **C5**, 2.00 μM; DNA, 3.00 μM (r=0.67, solid line) and 15.7 μM (r=0.13, dashed line). (c) **C7**, 3.17 μM; DNA, 3.85 μM (r=0.82).

from the theoretical curve (Fig. 5), and the CD changes describe a second binding step which is not detected by the absorbance changes (Fig. 3). When two binding steps are distinct and can be treated separately, two n values are obtained independently from the break points (shown by arrows) of the dashed lines in Fig. 5. The n values (n_{CD}) thus estimated are summarized in Table 2.

In the case of **C3**, the larger n value (n_{CD}=0.41) was quite similar to that obtained from the absorbance change (n_{AB}= 0.43). Therefore, the n=0.17 step for **C3** is sensitive only to the conformational change in DNA. This situation is also applicable to **C5**, where the n_{CD}=0.15 step is detected only by CD.

Induced CD Spectra To clarify the binding modes of the porphyrin, induced CD spectra[9,27] were measured at varying concentrations of the DNA. As seen in Fig. 6, bisignate CD peaks were commonly observed for the porphyrins, suggesting that the porphyrin binds externally with self-stacking on the DNA surface. In the case of **C3** and **C5**, two-step binding is suggested by the ellipticity change (Fig. 5), but the peaks diminish only slightly at large DNA loads corresponding to the smaller n_{CD} steps, indicating that the self-stacked porphyrins still dominate in these steps.

The most obvious difference among the porphyrins is the signal intensity of the induced CD peaks. The positive and negative peaks in the **C3** spectra are almost twice as strong as those of **C5**, and more than ten-times stronger than those of **C7**. As we pointed out previously,[17,24] the intensity of the bisignate induced signals is proportional to the n value for cationic porphyrins. In the present case, however, the trend is reversed, and an unusual mode of binding appears to be taking place.

DNA Cleavage The photonuclease activity for **C3**, **C5**,

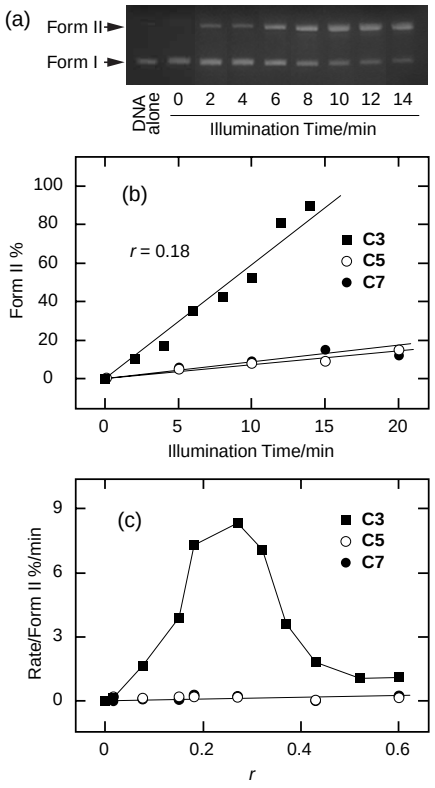

Fig. 7. Photonuclease Activity of Tentacle Porphyrins

(a) Agarose gel electrophoresis of plasmid DNA treated with 5.3 μM **C3**. Cleavage conditions: 30.0 μM pUC18 plasmid DNA in 10 mM sodium phosphate (pH 7.0) and 30% DMF, illumination at 420 nm at 25 °C. Form I and form II denote the supercoiled and nicked-circular forms of plasmid DNA, respectively. (b) Time course of the development of form II. Molar fraction of the form II is plotted against the illumination time. Porphyrin concentration was 5.3 μM (r=0.18). Closed squares, **C3**; open circles, **C5**; closed circles, **C7**. (c) Cleaving rate of tentacle porphyrins plotted against r. Closed squares, **C3**; open circles, **C5**; closed circles, **C7**.

and **C7** was examined using supercoiled pUC18 plasmid DNA. A mixture of porphyrin and plasmid (30 μM) was illuminated in air at 420 nm. After illumination, conversion of supercoiled DNA (form I) to nicked-circular DNA (form II) was investigated by agarose gel electrophoresis. On generation of a single-strand break, form I is converted to form II, which migrates more slowly on the gel.

As seen in Fig. 7a, form II DNA is clearly produced following prolonged illumination. The molar fraction of form II was quantitated by densitometry, and plotted against illumination time in Fig. 7b. It is clear that the molar fraction of the form II increases linearly with time and thus with the light dose. Highly efficient cleavage by **C3** is readily apparent, while **C5** and **C7** are rather poor photonucleases. The conversion rates were determined from the slopes of the lines, and these are plotted against the porphyrin load in Fig. 7c. The activity of **C5** and **C7** remains very low even at r=0.6 (r is [porphyrin]/[DNA] ratio). On the other hand, the rate increases initially to the **C3** load, indicating that **C3** catalyzed the DNA cleavage. When larger amount of **C3** is loaded, however, the rate decreased and an inhibitory effect of bound **C3** is clear.

Discussion

DNA Binding We have synthesized a series of novel porphyrins having aminoalkyl tentacles, and analyzed their DNA binding properties and photonuclease activities. Through the absorption and CD measurements, the spectral characteristics of these DNA-bound tentacle porphyrins were found to be distinct from any other cationic porphyrins; 1) They exhibit very large hypochromicity (Fig. 2), 2) they perturb DNA structure minimally (Fig. 4), and 3) they produce inverted bisignate induced CD pattern (Fig. 6). Thus, we conclude these porphyrins engage in a novel mode of DNA binding as discussed below.

The large hypochromicity indicates that the π electrons of the DNA-bound porphyrins are highly perturbed. In accord with this, bisignate CD signals were induced, indicating that the porphyrins are self-stacked; a negative signal is expected when porphyrins intercalate between the DNA base pairs, and groove-bound porphyrins show a positive signal.[9,27] The bisignate signals were, however, inverted when compared with "normal" cationic porphyrins.[17,24] Positive/negative (+/−) peaks normally appear at shorter/longer wavelengths, and our tentacle porphyrins showed −/+ pattern. Self-stacked porphyrins have been assumed to be aligned along the DNA surface, with their peripheral cationic groups in the DNA groove (edge-on). Thus, the greater the number of porphyrins bound (larger n value), the stronger the induced CD signals.[17,24] In our case, however, the signal intensity decreased in the order **C3**>**C5**>**C7** as the n_{AB} value increases. Since the hypochromicities among the tentacle porphyrins are nearly the same (Table 1), the degree of stacking is expected to be similar. Thus, DNA-bound porphyrins are suggested to be highly disordered (aggregation), especially for **C7**.

The tentacle porphyrins are achiral, but CD signals are induced when they bind to DNA which of course is chiral. Thus, the orientation of the bound porphyrin relative to the DNA axis is a major determinant of the CD signature.[28] Although speculative, we propose here that the tentacle porphyrins stacked with their planar surfaces facing the DNA duplex. This binding mode well accounts for the spectral characteristics of our tentacle porphyrins.

When cationic porphyrins are stacked edge-on, the positively charged peripheral groups protrude into the DNA groove, and interact directly with base pairs. Accordingly, CD signals in the UV range, where DNA bases are the main contributors to the spectrum, are usually affected by porphyrin binding. In our tentacle porphyrins, however, the structural change in the DNA is minimal, suggesting that the amino groups do not interact with base pairs. The amino group is expected to be protonated at neutral pH, and hence able to interact favorably with the negatively charged phosphate groups. The longer hydrocarbon stem of **C7** is more flexible, and this allows a disordered mode of binding to DNA. The hydrophobic nature of the stem should facilitate aggregation (or pile-up) with large n values. The piled porphyrins may be located away from the DNA axis, and contribute only weakly to the induced CD.

Photonuclease Activity **C3** was an efficient photonuclease, and its activity depended linearly on the light dose and **C3** concentration (Fig. 7). The high efficiency may be attributed in part to the high affinity of **C3** for DNA (Table 2). The short hydrocarbon stem of **C3** is suitable for DNA binding. However, **C5** and **C7** have moderate affinities, and their low activities have to be explained by other mechanism(s).

The nuclease activity of **C3** approaches a maximum at

about $r=0.2$, and then decreases to zero at about $r=0.4$. These r values are similar to the n_{CD} value (Table 2), indicating that DNA binding and photonuclease activity are closely correlated. The $n=0.17$ step was detected only by CD spectroscopy. Since the induced CD spectra of **C3** at $r=0.2$ and 0.4 are similar, the binding mode for these steps is the same (Fig. 6). Thus, the electronic structure should be quite similar, and the $n=0.17$ step is not detected by absorption spectroscopy.

The face-on binding mode satisfactorily accounts for the inactivation process for **C3**. In the $r=0$—0.2 range, **C3** lands softly on the target DNA with self-stacking. At this stage, the outer **C3** is situated quite close to the DNA, it absorbs light, and generates active oxygen species. In the subsequent $r=0.2$—0.4 range, **C3** piles up and aggregates, further sequestering the inner **C3** species, and ultimately the nuclease activity is fully inhibited. The distant location of additionally piled **C3** in this range is supported by induced CD spectra (Fig. 6). The signal intensity at $r=0.2$ increases only slightly at $r=0.4$, although the **C3** load is almost doubled. The more remote location of the additional **C3** species from the DNA axis is expected to induce CD only weakly.

The tentacle porphyrins were found to have unique spectral characteristics, which are well explained by putative face-on stacking. The **C3** linker is effective in enhancing the binding affinity. The extended hydrocarbon stem of the tentacle, however, promoted piled-up aggregation, which is inhibitory to the photonuclease activity. Thus, non-aggregating tentacle porphyrins are likely to be more efficient photonucleases and therefore show greater promise in applications in cancer PDT.

Acknowledgments The authors thank Dr. Anthony J. Wilkinson, University of York, U.K., for valuable discussion. This work is supported by a grant for Science Research (13557199 to T. U.) from Japan Society for Promotion of Science.

References and Notes

1) Amitage B., *Chem. Rev.*, **98**, 1171—1200 (1998).
2) Ali H., van Lier J. E., *Chem. Rev.*, **99**, 2379—2450 (1999).
3) Fiel R. J., Datta-Gupta N., Mark E. H., Howard J. C., *Cancer Res.*, **41**, 3543—3545 (1981).
4) Praseuth D., Gaudemer A., Verlhac J.-B., Kraljic I., Sissoeff I., Guille E., *Photochem. Photobiol.*, **44**, 717—724 (1986).
5) Dougherty T. J., *Photochem. Photobiol.*, **58**, 895—900 (1993).
6) Fiel R. J., *J. Biomol. Struc. Dyn.*, **6**, 1259—1274 (1989).
7) Pasternack R. F., Gibbs E. J., *Met. Ions Biol. Syst.*, **33**, 367—397 (1996).
8) Marzilli L. G., *New. J. Chem.*, **14**, 409—420 (1990).
9) Pasternack R. F., Gibbs E. J., Villafranca J. J., *Biochemistry*, **22**, 2406—2414 (1983).
10) Fiel R. J., Howard J. C., Mark E. H., Datta Gupta N., *Nucleic Acids Res.*, **6**, 3093—3118 (1979).
11) Carvlin M. J., Fiel R. J., *Nucleic Acids Res.*, **11**, 6121—6139 (1983).
12) Carvlin M. J., Mark E. H., Fiel R. J., *Nucleic Acids Res.*, **11**, 6141—6154 (1983).
13) Sari M. A., Battioni J. P., Dupre D., Mansuy D., Le Pecq J. B., *Biochemistry*, **29**, 4205—4215 (1990).
14) Sehlstedt U., Kim S. K., Carter P., Goodisman J., Vollano J. F., Norden B., Dabrowiak J. C., *Biochemistry*, **33**, 417—426 (1994).
15) Marzilli L. G., Banville D. L., Zon G., Wilson W. D., *J. Am. Chem. Soc.*, **108**, 4188—4192 (1986).
16) Guliaev A. B., Leontis N. B., *Biochemistry*, **38**, 15425—15437 (1999).
17) Uno T., Aoki K., Shikimi T., Hiranuma Y., Tomisugi Y., Ishikawa Y., *Biochemistry*, **41**, 13059—13066 (2002).
18) Bütje K., Nakamoto K., *Inorg. Chim. Acta*, **167**, 97—108 (1990).
19) Ishikawa Y., Yamakawa N., Uno T., *Bioorg. Med. Chem.*, **10**, 1953—1960 (2002).
20) Yamakawa N., Ishikawa Y., Uno T., *Chem. Pharm. Bull.*, **49**, 1531—1540 (2001).
21) Ishikawa Y., Yamashita A., Uno T., *Chem. Pharm. Bull.*, **49**, 287—293 (2001).
22) Scatchard G., *Ann. N.Y. Acad. Sci.*, **51**, 660—672 (1949).
23) Correia J. J., Chaires J. B., *Methods Enzymol.*, **240**, 593—614 (1994).
24) Uno T., Hamasaki K., Tanigawa M., Shimabayashi S., *Inorg. Chem.*, **36**, 1676—1683 (1997).
25) http://rsb.info.nih.gov/nih-image/
26) Nielsen P. E., Jeppesen C., Egholm M., Buchardt O., *Biochemistry*, **27**, 6338—6343 (1988).
27) Pasternack R. F., Garrity P., Ehrlich B., Davis C. B., Gibbs E. J., Orloff G., Giartosio A., Turano C., *Nucleic Acids Res.*, **14**, 5919—5931 (1986).
28) Kubista M., Åkerman B., Nordén B., *J. Phys. Chem.*, **92**, 2352—2356 (1988).